EIGHTH EUROPEAN ROTORCRAFT FORUM

Paper No. 11.7

BO 105 ROTOR BLADE INFLUENCE ON THE CALIPSO FLIR IN THE MAST-MOUNTED OBSERVATION PLATFORM OPHÉLIA

H.-D.V. BÖHM

MESSERSCHMITT-BÖLKOW-BLOHM GmbH

MUNICH, GERMANY

August 31 through September 3, 1982

AIX-EN-PROVENCE, FRANCE

ASSOCIATION AERONAUTIQUE ET ASTRONAUTIQUE DE FRANCE

Bo 105 rotor blade influence on the CALIPSO FLIR in the mast-mounted observation platform OPHÉLIA

H.-D.V. Böhm
Messerschmitt-Bölkow-Blohm GmbH
Munich, Germany

Abstract

The mast-mounted observation platform OPHÉLIA (MMO) was tested on the MBB helicopter Bo 105-S1. This visionics system includes a FLIR, CALIPSO, based on the French Common Module Programme (SMT). The CALIPSO FLIR has two fields of view (FOV) and a serial-parallel scan mechanism. In flight, when the stabilized platform containing the FLIR is directed downwards at an elevation (El) of - 10.4° to look through the main rotor blades, the influence of the blades on the thermal image can be seen in the centre of both FOV.

This paper presents a description of the MMO and FLIR and gives a theoretical discussion based on the geometry of the total system, considering first the static and then the dynamic case. It can be seen from flight tests and theoretical discussion that, for this combination, the rotor blade influence on both FLIR FOV is small and relatively insignificant. The background thermal image remains virtually unobscured under rotor blade influence.

The latter part of the paper presents a theoretical discussion of rotor blade influence on different types of FLIR system.

Introduction

During the period May 1981 - Jan. 1982, an experimental programme, sponsored by the German Ministry of Research and Technology (BMFT) was carried out by MBB using a Bo 105 as flying test bed. The OPHÉLIA experiment was performed to test a mast-mounted observation platform installed above the rotor head. The platform houses the CALIPSO FLIR, a TV camera and a laser range-finder (ref. 1, 2 and 3). One of the aims of this MMO experiment was the determination of the rotor blade influence on the CALIPSO FLIR.

The rotor blade influence depends, in general, on the following parameters:

- scan speed of the FLIR mirror or polygon
- scan mechanism (parallel, serial-parallel or serial)
- size of the FOV
- rotor speed
- distance of the mast-mounted FLIR sight from the rotor disc
- width of the rotor blades
- number of rotor blades and
- LOS (line of sight) angle of the FLIR through the rotor blades

The dimensions of the integrated mast-mounted observation platform and the type of scan mechanism used in the FLIR are the main factors in the analysis of rotor blade influence. Tests to determine rotor blade influence were carried out in flight and during ground running.

2. Geometrical description of OPHÉLIA and technical aspects of the CALIPSO FLIR

The chief parameters of the stabilized platform, provided by SFIM, are:

- o two axes stabilized platform, gyro stabilized with two stages: coarse stabilization with torquer, fine stabilization with mirror
- o approx. 600 mm platform diameter
- o displacement angles: azimuth ± 120°
  elevation - 30°/+ 20°
- o slew rate approx. 10°/s

Fig. 1 shows the helicopter with the MMO. A stationary stand pipe (30 mm ∅) containing electrical wires and two cooling tubes, leads through the rotor hub to the bottom of the gear box.

The distance from the rotor disc to the LOS plane of the FLIR is 1100 mm. Fig. 2 shows the platform installation, while dimensions are given in Fig. 3. The Bo 105 has four equi-spaced main rotor blades. The width of each blade is approx. 270 mm over its total length. The diameter of the rotor disc is 9.8 m, with an in-built coning angle of 2.5°. The rotor has a nominal speed of 44.4 rad/s (advancing blade on the starboard side), giving an approx. rotor frequency of 7 Hz.

Fig. 1: Bo 105-S1 with the mast-mounted observation platform, OPHÉLIA

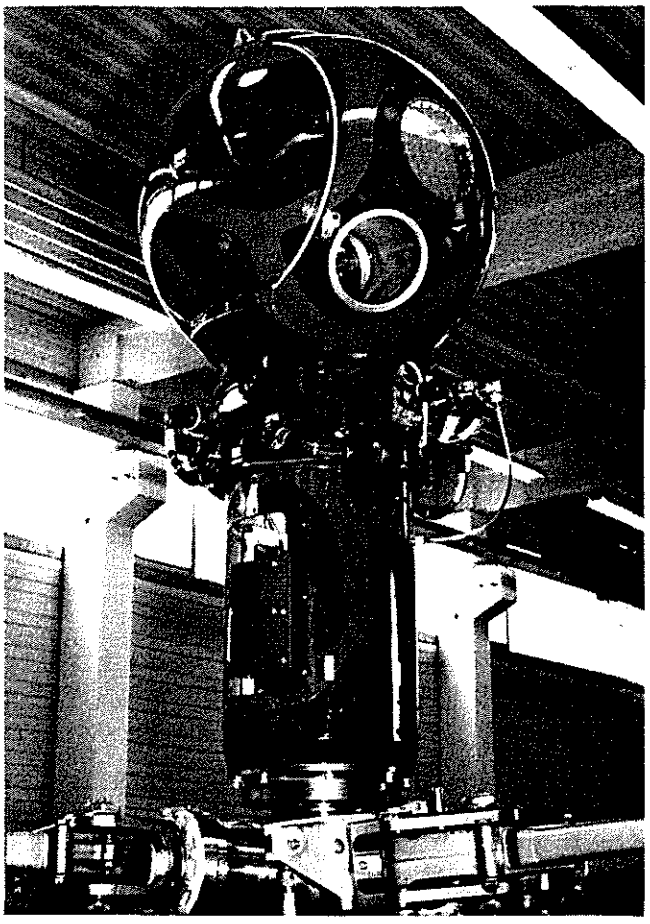

Fig. 2: Stabilized OPHÉLIA platform on the rotor head with sensc package installed

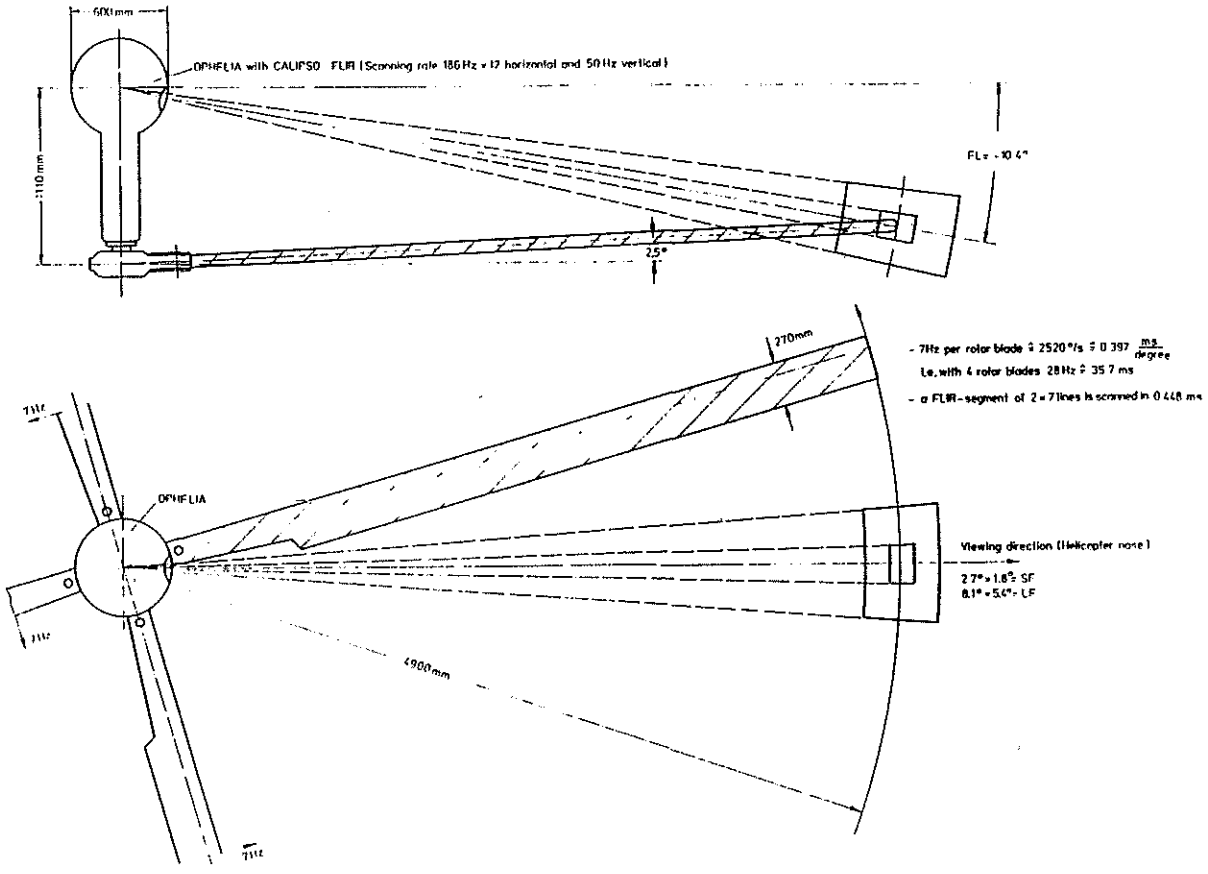

Fig. 3: Dimensions and the static influence of the Bo 105 rotor blades on the LF and SF of the CALIPSO FLIR, installed in the MMO (OPHÉLIA) 11.7/4

The characteristics of the CALIPSO FLIR with French SMT, provided by TRT, are listed below:

- o two FOV: 5.4° x 8.1° (4 x magn.), called LF, IFOV = 0.36 mrad
  1.8° x 2.7° (12 x magn.), called SF, IFOV = 0.12 mrad
- o field rate 50 Hz, frame rate 25 Hz
- o spectral range 8 - 13 µm
- o EP = 155 mm and f_{eff} = 417 mm
- o open cooling system with nitrogen bottle for cooling the CdHgTe-detectors (Joule Thomson Principle)
- o scan mechanism serial-parallel
- o approx. 504 lines per frame rate
- o 7 lines and 6 detectors per line
- o 42 detectors with 50 µm x 50 µm size: 6 x 7 matrix
- o 12-faced rotating mirror with approx. 186 Hz scanning frequency or 2232 Hz per FOV for 7 lines (18079°/s)
- o one scan over the FOV with 7 lines takes 0.448 ms. This is calculated not taking into account a scan efficiency of 93 %
- o the vertical image scanning is provided by a tilt mirror operating at 50 Hz and 82 % scan efficiency

Fig. 4 shows the CALIPSO FLIR with associated electronic box. This box is installed in the helicopter cargo bay and not in the platform.

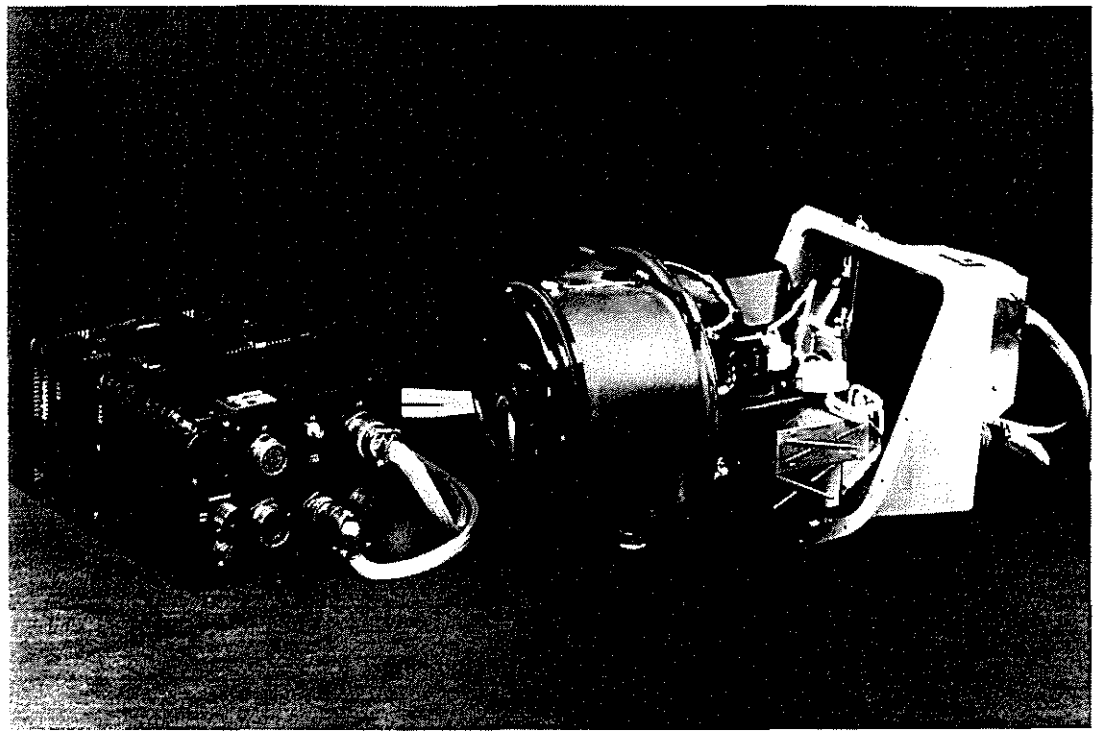

Fig. 4: CALIPSO FLIR, provided by TRT, with electronic box and serial-parallel scanning mechanism

The two displays, provided by VDO, are shown in Fig. 5 under simulated night conditions. The lower part of the picture shows the Head-down Display (HDD), together with controls, on which is displayed a thermal image. The thermal image displayed on the Head-up Display (HUD), in the upper part of the picture, is out of focus owing to the fact that in a HUD the image is focused at infinity. In this case, the camera taking the photo was focused to approx. 1 m.

The visionics system described has two symbologies. One symbology is provided by SFIM to give information on platform displacement and sensor setting, the other is provided by VDO/MBB to give the pilot flight information.

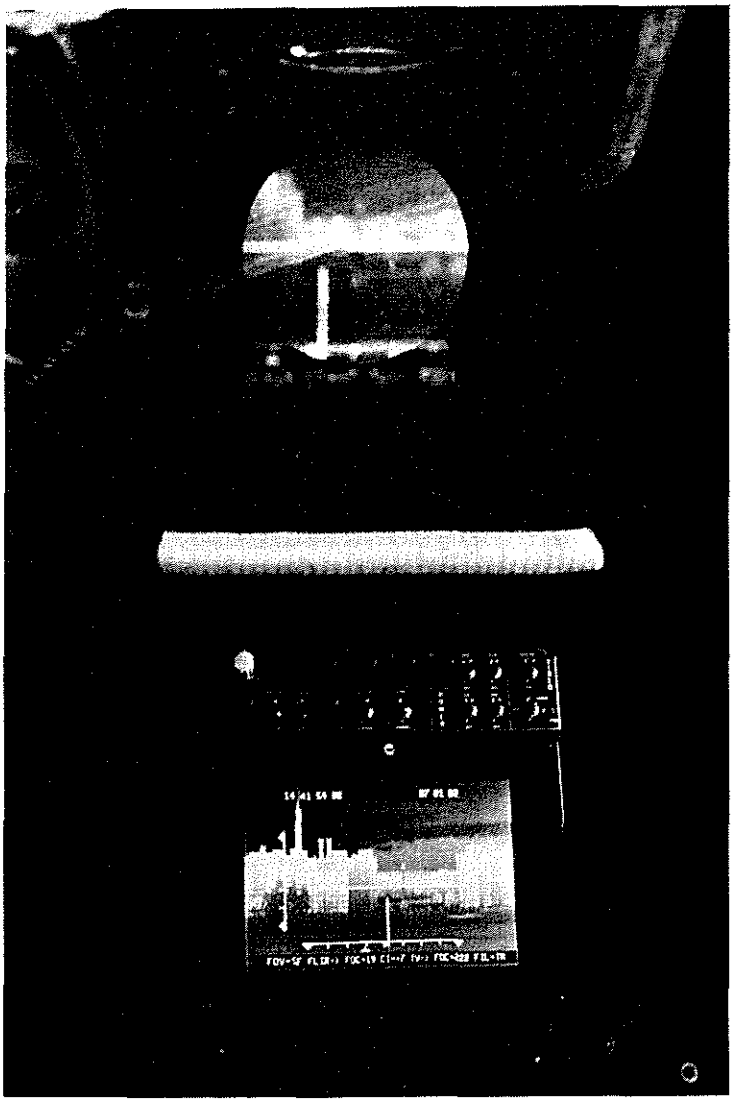

Fig. 5: HUD (above) and HDD (below) with thermal image by simulated night

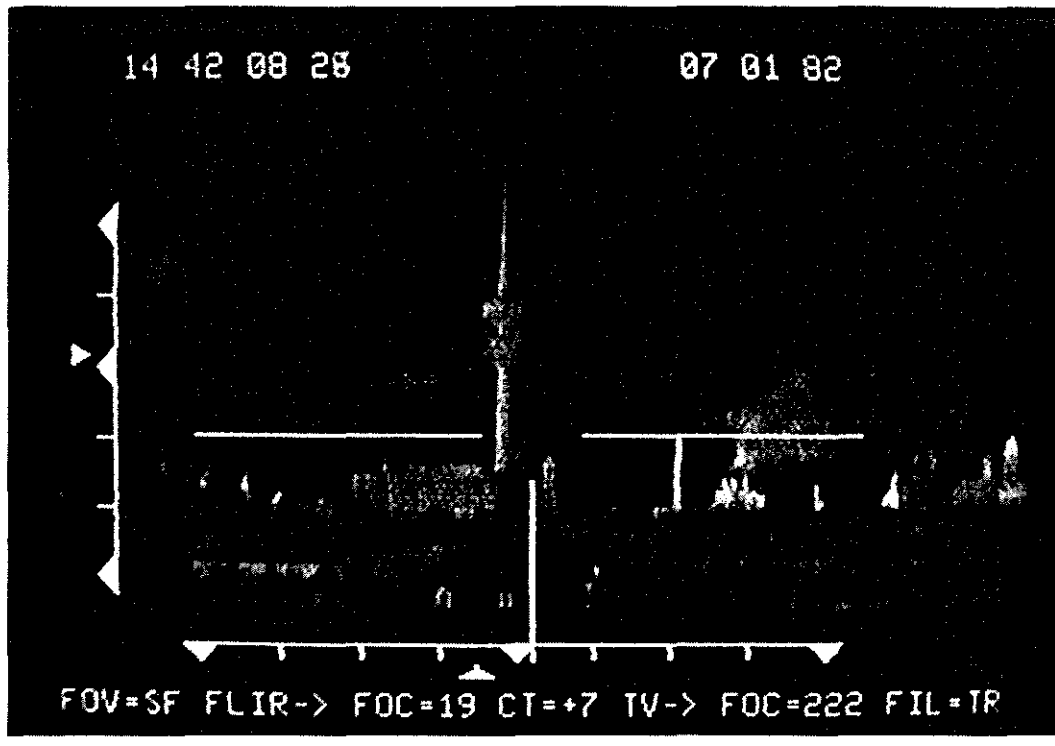

Fig. 6: Thermal image of the Munich Olympic Tower at a distance of 16 km taken with the CALIPSO FLIR

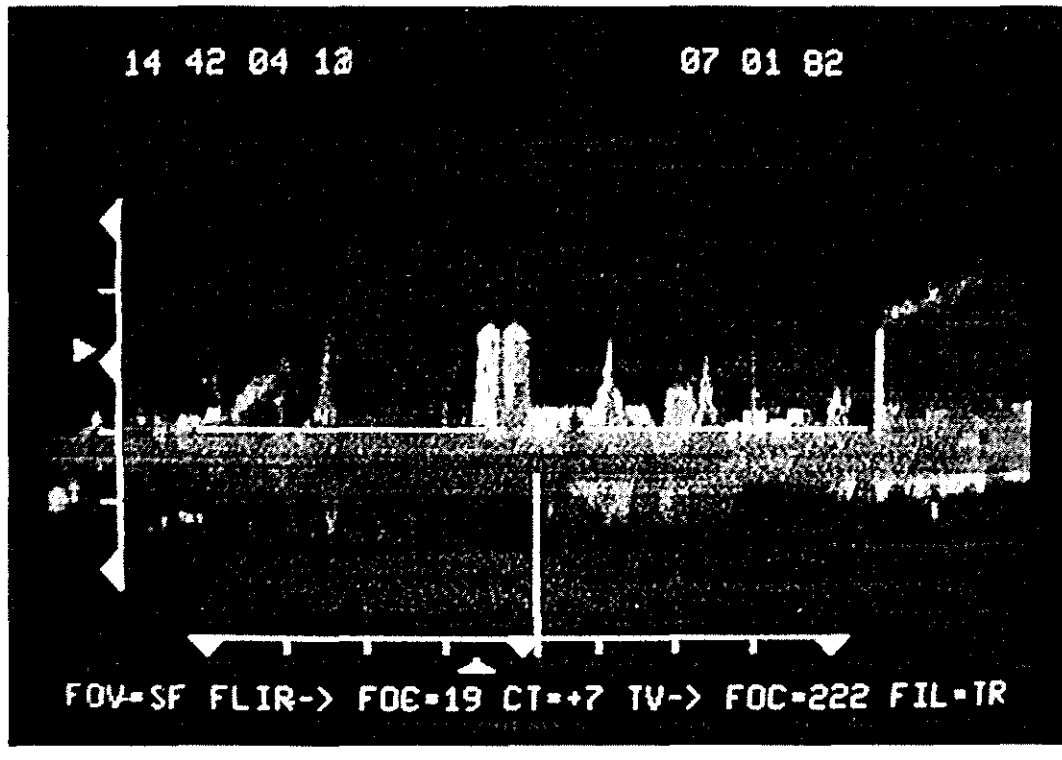

Fig. 7: Thermal image of the Munich Frauenkirche at a distance of 11.7 km taken with the CALIPSO FLIR

Fig. 6, Fig. 7 and subsequent photos show the SFIM symbology with platform displacement (Az: 30°/scale division, El: 10°/scale division), time (upper left), date (upper right) and an information band (below) with FOV, FLIR focus, FLIR contrast and TV camera information.

Fig. 6 shows the Munich Olympic Tower at a distance of 16 km and Fig. 7 the Munich Frauenkirche at 11.7 km distance. Both of these thermal images were taken on the 7th Jan. 1982 at 14:42 h in good weather conditions. The IR visibility was considerably better than the 0.5 µm visibility.

3. Static consideration of a video field (20 ms) with stationary and rotating blades, taken with the CALIPSO FLIR

Fig. 8 shows a stationary rotor blade in the large field of view (LF) of the FLIR image for a static video field. The rotor blade is aligned with the helicopter longitudinal axis and can be seen directly in the centre of the thermal image.

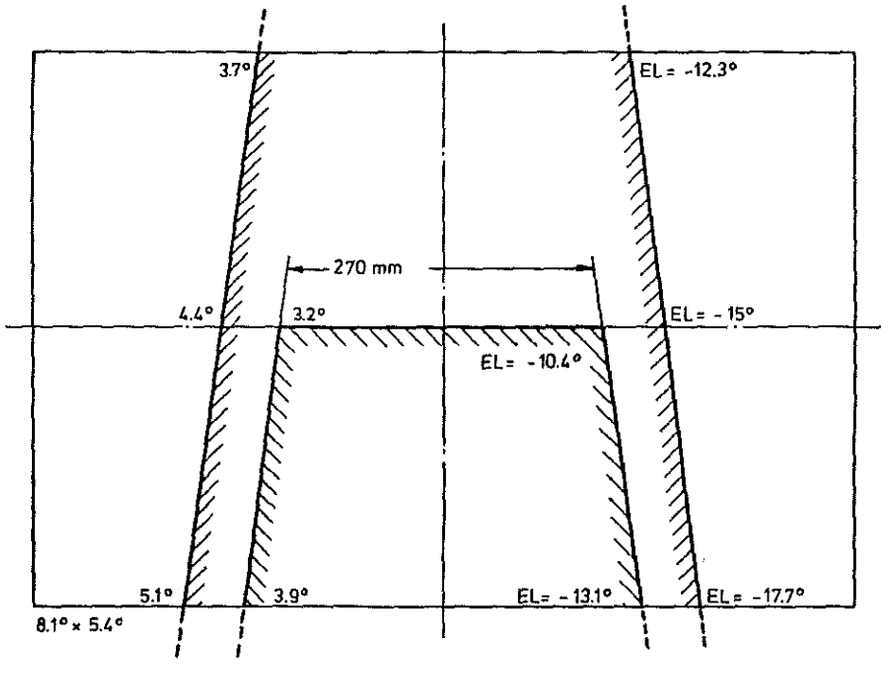

Fig. 8: Static video field with a stationary rotor blade in the centre. 1st LOS at El = - 10.4°, 2nd LOS at El = - 15°, both for the LF

If the LOS of the FLIR is directed downwards at - 10.4° El, the rotor blade covers only the lower part of the picture and the tip of the blade is seen in the centre of the image. If, however, the FLIR LOS is directed at - 15° El, the thermal image shows the rotor blade, in perspective, over the total picture height.

If the rotor rotates at 100 % (7 Hz), the four blades do not, however, obscure the total vertical field of the thermal image. The reason for this is provided by the differing speeds of the FLIR scan mechanism and the blades. In addition, the CALIPSO FLIR scans from left to right at approx. 18079°/s while the blades rotate counter-clockwise at approx. 2520°/s.

During the image synthesis of one line package, one rotor blade moves 2520°/s x 0.448 ms = 1.129°. This means that, considering the static video field of 20 ms, the rotor blade is cut into steps. In the LF there are 8.1° : 1.129° = 7.2 steps per video field, in the case of one rotor blade intersecting the 20 ms static image. The step angle is approx. 7.6° in the LF (El = - 15°). However, as the rotor blade is not a theoretical thin line (270 mm width), it is possible to detect more than 7.2 steps in the LF. These additional steps are shown in Fig. 9. The number of additional steps depends on the FLIR LOS and the FOV.

If the FLIR is directed at - 15° El, one rotor blade covers 4.4° of the 8.1° image width (Fig. 8). This results in 4 additional steps. Blurring is seen on the left and right edges of each step. For the same angle of elevation of - 15° in the SF (2.7°), the blade also covers 4.4°, but produces a SF image disturbance of approx. 2.4 steps in the static video field.

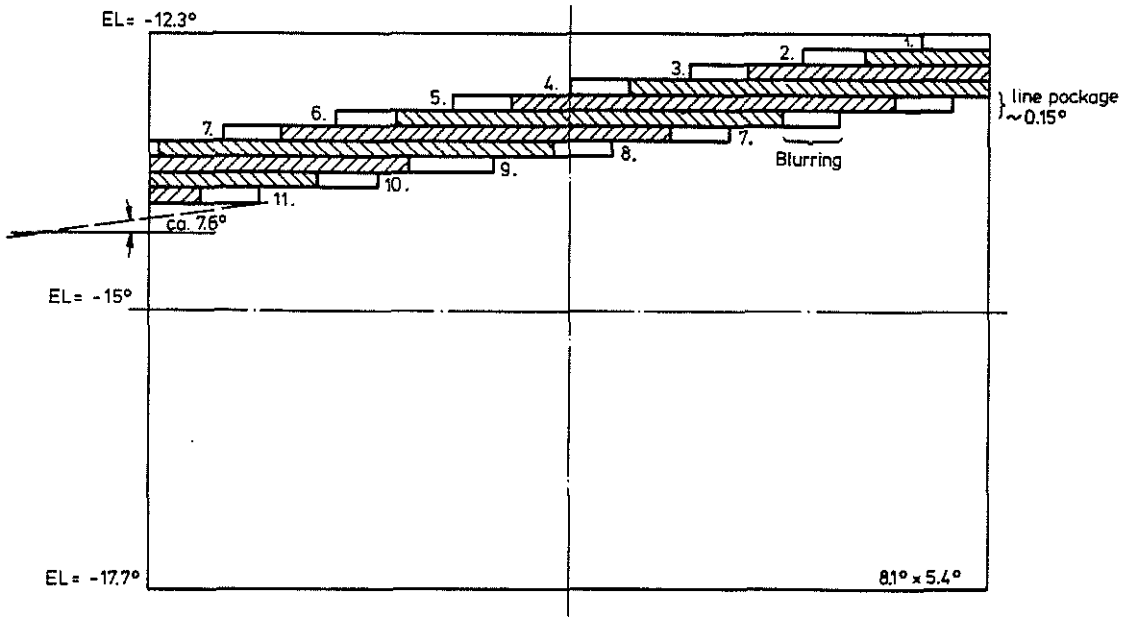

Fig. 9: Static video field with 100 % rotor speed. LOS is at El = - 15° in the LF. The serial-parallel FLIR scan mechanism cuts the rotor blade image into steps.

Fig. 10 shows the rotor blade influence on the LF. The hot rotor blade, white in the picture, is seen in the static video field of 20 ms. This thermal image was taken during ground running on the 18th Aug. 1981 at 20:15 h local time and shows the 49th video field. The FLIR LOS is at El = - 15°. The conditions in the thermal image with the distorted rotor blade conform well with the theory discussed above.

In Fig. 11 the rotor blade is cut into approx. 11 full steps instead of 7.2 steps. During this ground run, the main rotor was running at approx. 70 % of nominal speed. At this rotor speed, the blade rotates only 0.79° per line package of 7 lines instead of 1.129°. The step angle is now approx. 10.8° and the blade distortion is less than in Fig. 10.

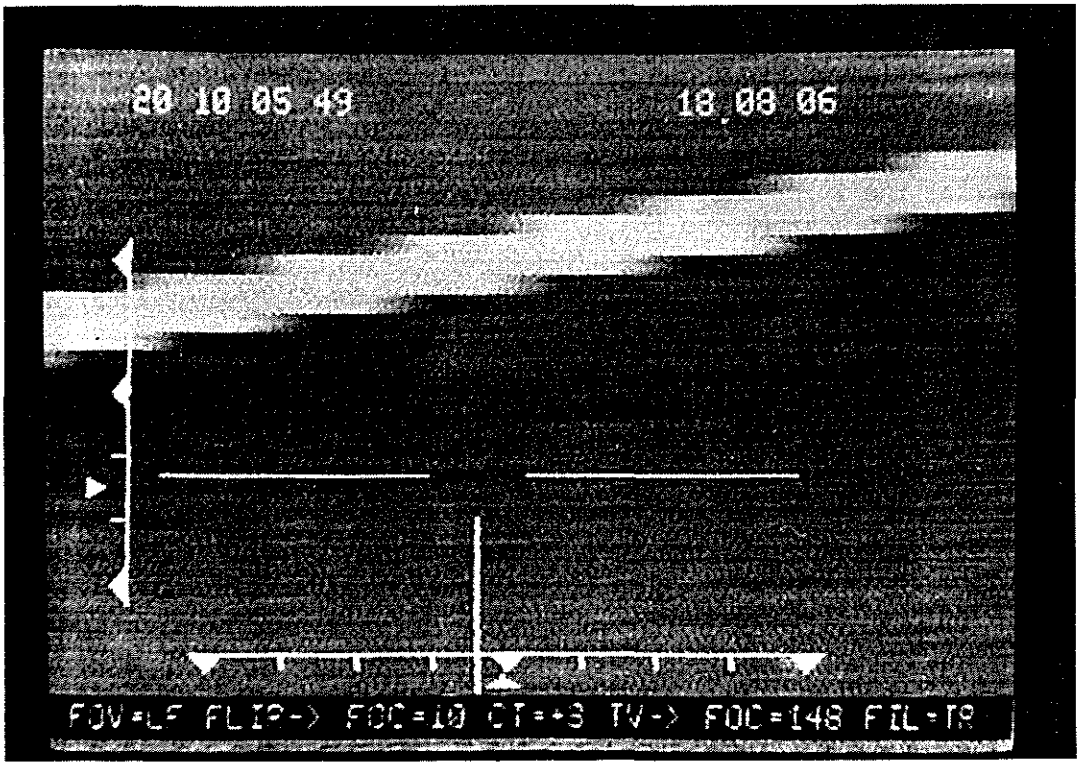

Fig. 10: Thermal image with rotor blade influence at 100 % rotor speed. This picture shows a static video field of 20 ms. The FLIR LOS is at El = - 15° in the LF. The rotor blade image is cut into approx. 7.2 steps.

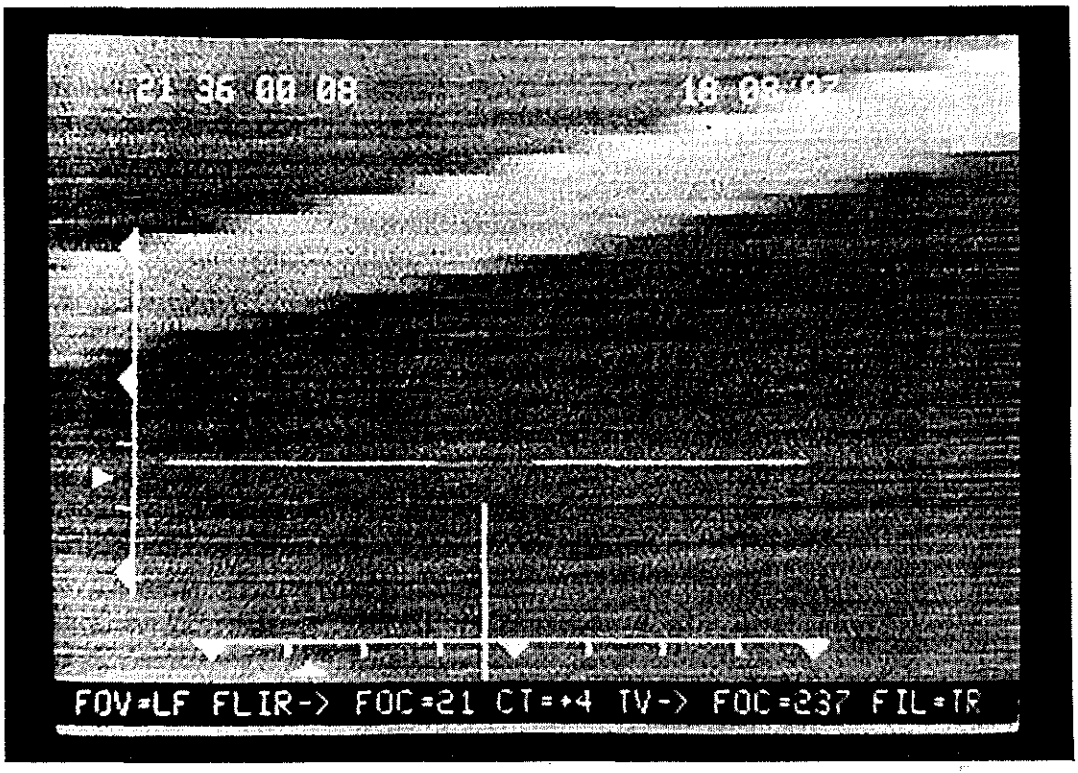

Fig. 11: Thermal image with rotor blade influence at 70 % rotor speed. This picture shows again a static video field of 20 ms. The FLIR LOS is at El = - 15° in the LF. The rotor blade image is cut into approx. 11 steps.

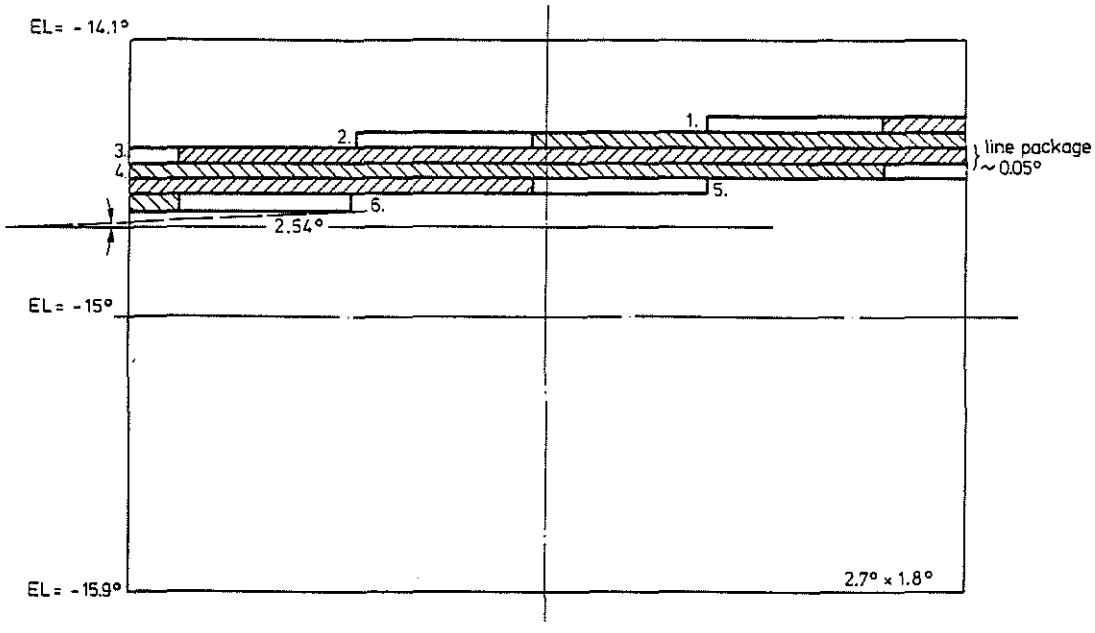

Fig. 12: Static video field at 100 % rotor speed. The LOS is at El = - 15° in the SF. The serial-parallel FLIR scan mechanism cuts the rotor blade image at this angle of elevation into approx. 2.4 steps, without blurring.

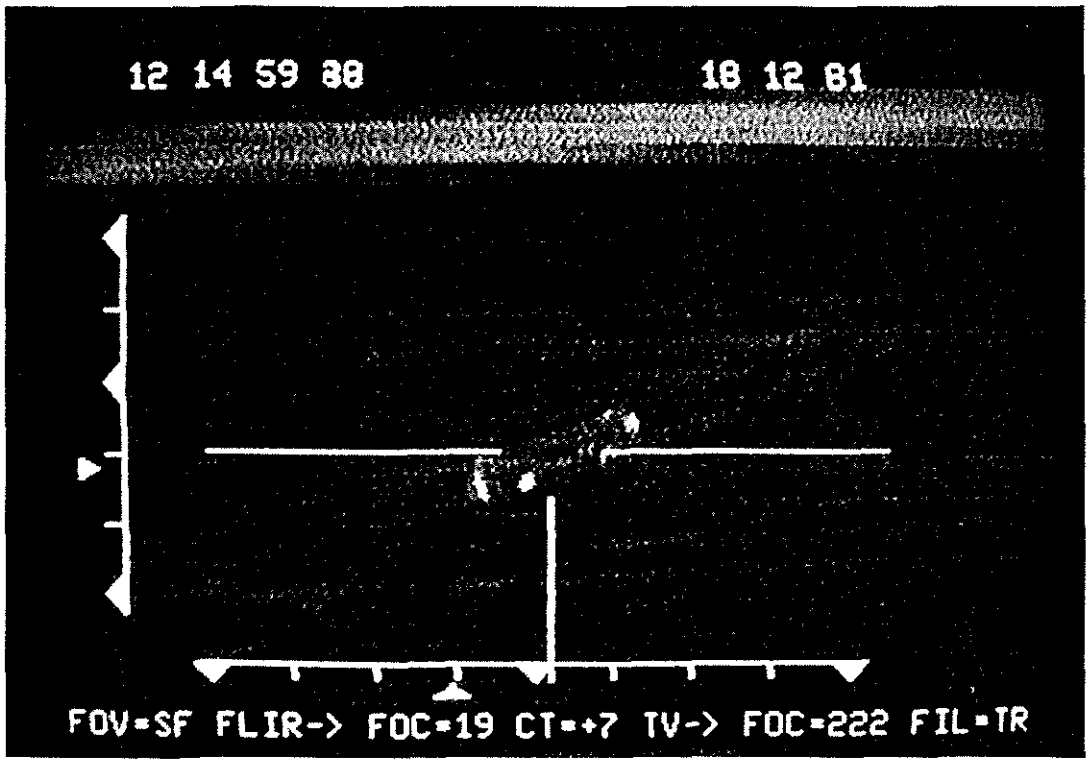

Fig. 13: Thermal image with rotor blade influence at 100 % rotor speed. This picture shows a static video field of 20 ms. The FLIR LOS is at El = - 12° in the SF. The rotor blade image is cut into approx. 2 full steps.

In the small field of view (SF) with 2.7° x 1.8°, the rotating blade appears much more distorted and blurred. Fig. 12 shows a static video field with 100 % rotor speed. At this constant rotation, a blurring of 1.129° occurs, the same as in the LF, but the blurring per picture width in the SF is nearly 3 x more than in the LF. In the SF there are 2.7° : 1.129° = 2.4 steps, with a step angle of 2.54°.

Fig. 13 shows the rotor blade influence during a flight test using the SF of the CALIPSO FLIR. In this thermal image, the El angle of the FLIR LOS is approx. - 12°. The helicopter is performing a roll maneouvre. The photo also shows a large vehicle at 1.8 km distance. The scanning steps of the segmented rotor blade image are more blurred than in the LF. Fig. 13 also shows that the rotor blade influence on the SF on the static video field is smaller than that on the LF (see section 4).

4. Dynamic consideration of several video fields with blade rotation for the CALIPSO FLIR

In the last section we considered one static video field of 20 ms duration under the influence of a rotor blade. In this section we shall consider the dynamic effect of several video fields. It will subsequently be shown that not every video field is affected.

Fig. 14 demonstrates the dynamic effect in the LF. It shows 5 separate video fields with a marked time scale. In this presentation, the rotor blade influence on each field can easily be seen. The tilt mirror for the vertical scanning has a dead time of approx. 3.9 ms (82 % scan efficiency). The 1st video field shows a rotor blade after 6 ms, which we label as the 1st blade. The blade image has the afore-mentioned step angle of 7.6° for the LF and 2.6° for the SF (section 3). At nominal speed, the 2nd of the 4 rotor blades is in exactly the same position as the 1st blade after 35.7 ms. Because each video field has a duration of 20 ms, the 2nd blade can be seen slightly shifted in the 3rd video field. The 3rd blade arrives at the same position as blade 1 after 71.4 ms. This blade is seen partly in the dead time of the 4th field and partly in the 5th field.

Fig. 15 shows 8 superimposed video fields (160 ms), conforming to CCIR standard, with the rotor blade influence at a constant FLIR LOS of El = - 15° in the LF. The drawing shows the effect of the rotor blade. When viewed in real-time on a TV-monitor, the effect of the blades is not as marked as shown in Fig. 15. The eye has an image-processing time of 0.2 s, while we are here theoretically considering only 0.16 s of a video tape. If there is an object in the thermal image, it can always be seen during rotor blade influence.

In the SF, the blade rotation time is the same as in the LF. However, the step angle changes to 2.4° and the dwell time of the rotor blades is shorter. This latter effect is the reason why the blade influence is less in the SF than in the LF.

A simple calculation of rotor blade disturbance at El = - 15° is now given for the LF. At a rotor frequency of 7 Hz, one blade, considered theoretically as a thin line, is seen for 3.2 ms in the 8.1° image width. For the actual 270 mm wide blade an additional time of 1.7 ms has to be included. At El = - 15°, the total dwell time in the LF is approx. 4.9 ms (without blurring effect).

The 2nd blade follows after 35.7 ms. This results in a rotor blade disturbance, for this angle of elevation, over a maximum of 14 % of the time. This time is slightly reduced if the horizontal and vertical scan efficiencies (or dead time) are taken into account. It should be stressed, that only certain of the line packages, which make up the image, are approx. 14 % vignetted and not the whole image!

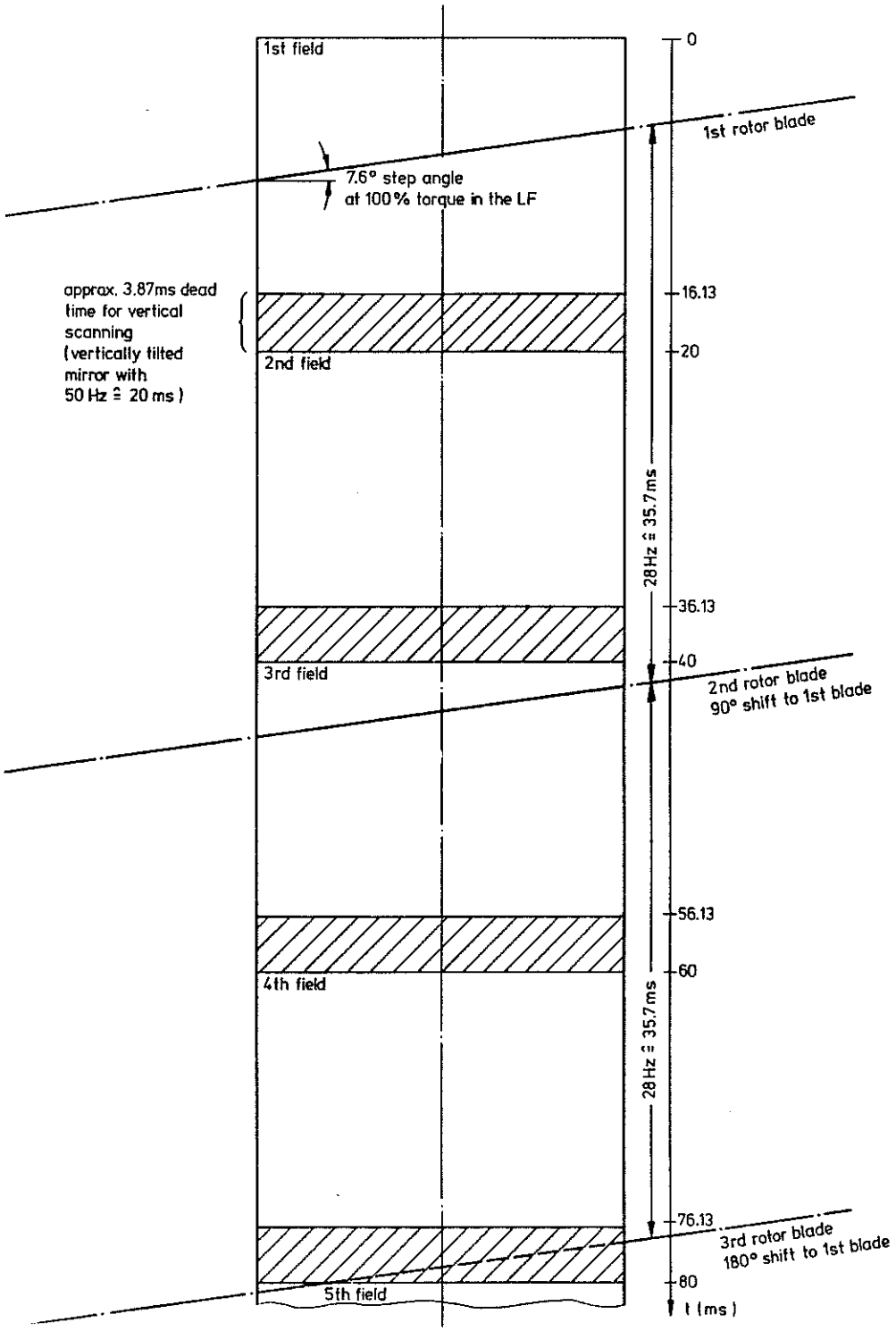

Fig. 14: Rotor blade influence on 5 separate video fields (100 ms) for the LF. (For explanation, see text).

In the SF (2.7°) a thin line rotor blade is seen for only 1.1 ms. For a real rotor blade at El = - 15°, 1.7 ms has to be added, giving a total disturbance of 2.8 ms. When related to the 35.7 ms between two rotor blades, the blades have an influence on the image over approx. 8 % of the time. Of this 8 %, only certain of the line packages are vignetted and not the whole image!

Considering a FOV of 30° x 45° for a pilot's FLIR, the time disturbance is max. 55 % (without scan efficiency correction).

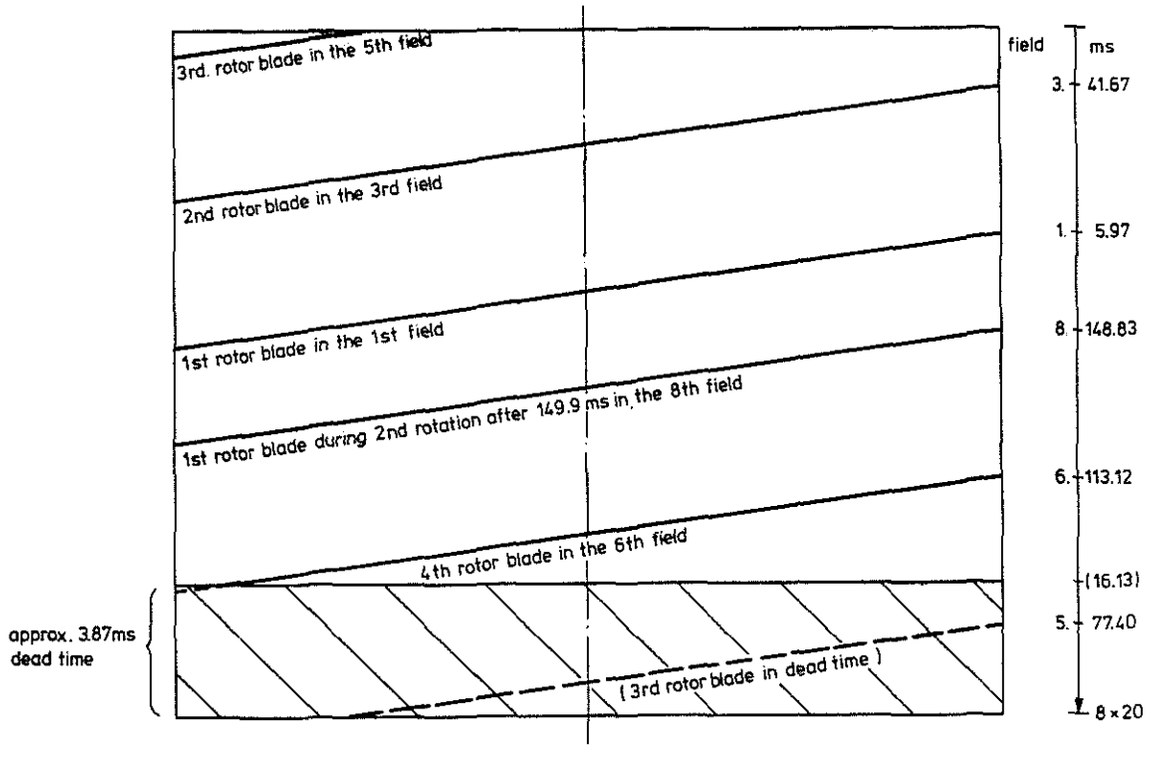

Fig. 15: Rotor blade influence demonstrated with 8 superimposed video fields (160 ms). In the dynamic case approx. 14 % of the LF image and 8 % of the SF image are vignetted in time, with only certain line packages, and not the whole image, being vignetted.

Fig. 16 shows a thermal image in the LF taken during flight tests. The picture was taken from a monitor while a video tape of the flight tests was running. A camera with an exposure time of 1/15 s (0.067 s) was used. The European TV standard shows slightly more than 3 video fields. This picture has been selected from numerous pictures, in which the effect of the 1st rotor blade is seen in the 1st video field and the 2nd rotor blade in the 3rd video field (see also Fig. 14). In the background there are clouds.

Fig. 17 also demonstrates the rotor blade influence with 3 video fields in the thermal image in the LF. In this picture we can see a hot chimney with smoke in the background. In spite of the rotor blades, the complete chimney is visible.

To summarise, the rotor blade influence in both the LF and the SF of the CALIPSO FLIR is relatively small. Flight tests with video recordings have substantiated theoretical calculations. The objects under observation can still be seen through the rotating blades with this serial-parallel scanning mechanism Only a slight "chopper" effect is noticed by the observer.

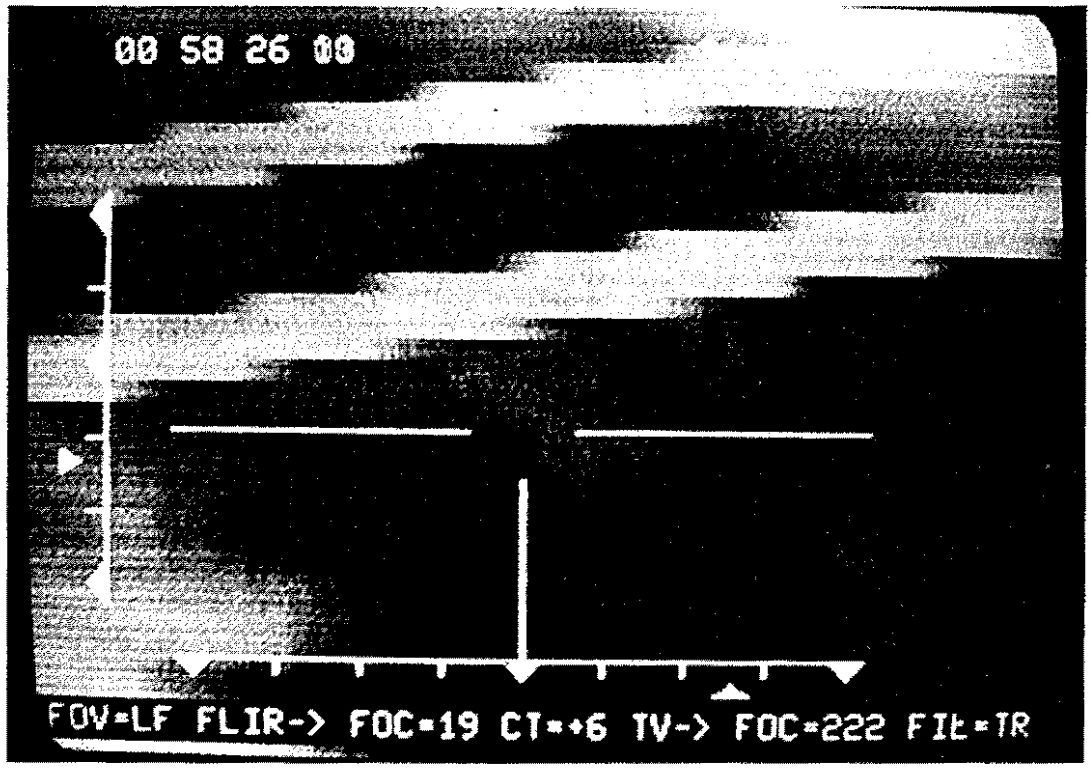

Fig. 16: Thermal image with rotor blade influence in the LF during flight tests. Three video fields were exposed while a camera recorded the image from a video tape on a monitor. El = - 13°. In the background are clouds.

Fig. 17: Thermal image with rotor blade influence in the LF during flight tests. El = - 11°. In spite of the rotor blades, the complete chimney (hot), with smoke, is visible.

5. Rotor blade influence with different FLIR scanning mechanisms; parallel and serial

FLIR with parallel scanning

A FLIR based on American Common Modules (CM) has a parallel scanning mechanism with a 2:1 interlace and either 60, 120 or 180 detectors vertically in line. In order for the CM FLIR to obtain a picture the width of the FOV in one scan, using American video standard, 1/120 s is required (ref. 4).

At the 2nd scan (interlace) the horizontal mirror changes scan direction. The scan mirror moves for 1/120 s with and, for the next 1/120 s, against the direction of blade rotation. With the serial-parallel scanning mechanism of the 12-faced CALIPSO polygon, the scan direction does not change and always runs against the direction of blade rotation. In contrast to the CALIPSO FLIR image, the rotor blade in the image produced by the CM FLIR with parallel scanning mechanism is not cut into segments.

Fig. 18 shows the synthesised dynamic and static cases for a Bo 105 rotor blade in the centre of an image taken with a CM FLIR for three superimposed stationary video fields (US stand). The FLIR FOV is taken to be 8.1° x 5.4° and the dimensions of the mast-mounted installation are the same as described in section 2. The FLIR LOS direction is again taken to be El = - 15°.

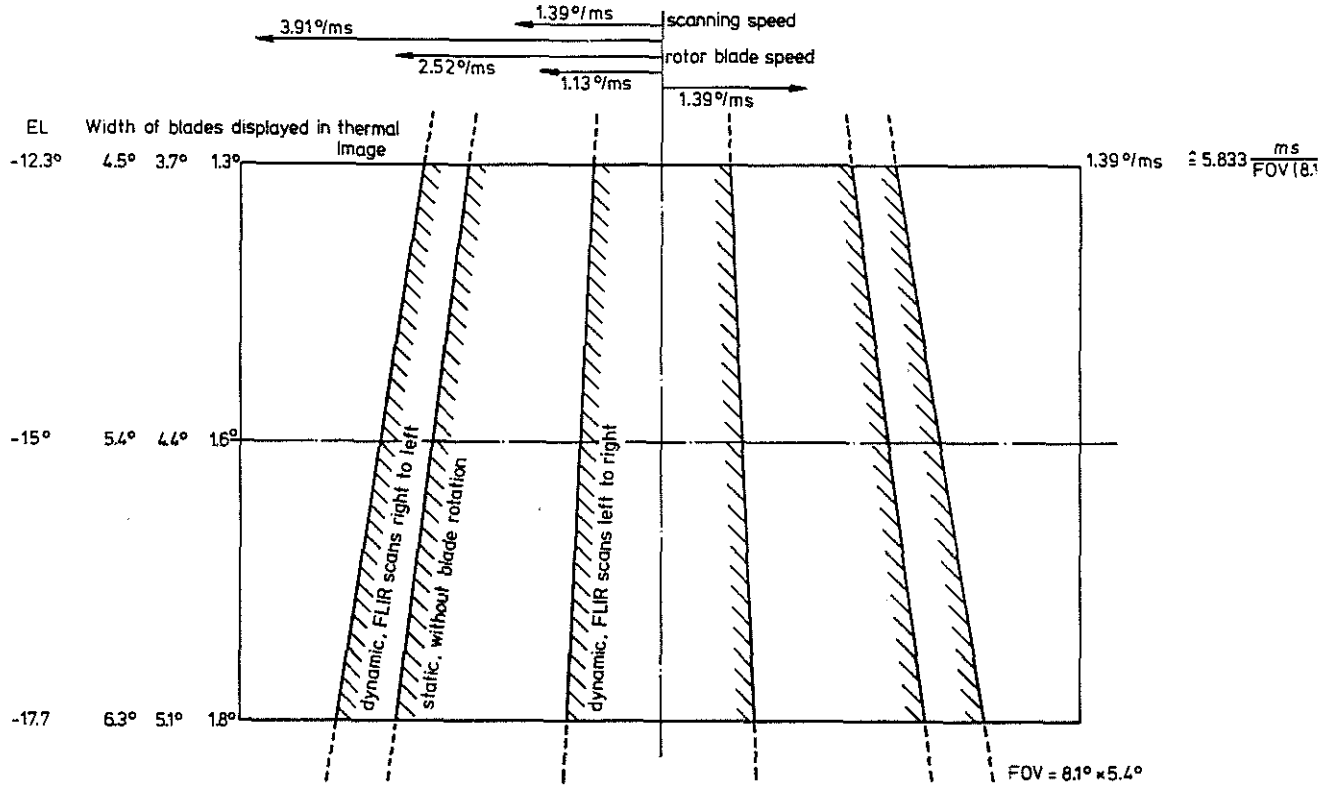

Fig. 18: Synthesis of static and dynamic cases for a rotor blade in the centre of an image taken with a CM FLIR for three superimposed stationary video fields.

The presentation of the static case (without blade rotation) and the two dynamic cases (with blade rotation), which show scanning with and against direction of blade rotation, are only valid if the blade is seen in the centre of the image in each video field. A stationary video field image of the two dynamic cases shows the rotor blade cut into very small segments with one video line missing (interlace effect), not shown in Fig. 18. The eye cannot, however, detect this in a running video tape. The upper part of Fig. 18 shows the speeds of a Bo 105 rotor blade and of the CM FLIR scanning device. These are 2.52°/ms and ± 1.39°/ms (to the left or right) respectively. When added, these result in speeds for the image synthesis of a rotor blade of 3.91°/ms or 1.13°/ms. As a comparison, it should remembered that the scanning speed of the CALIPSO FLIR was 18.1°/ms instead of 1.39°/ms. The width of blades displayed in the stationary video field (static and dynamic cases) is shown for different elevation angles in the image.

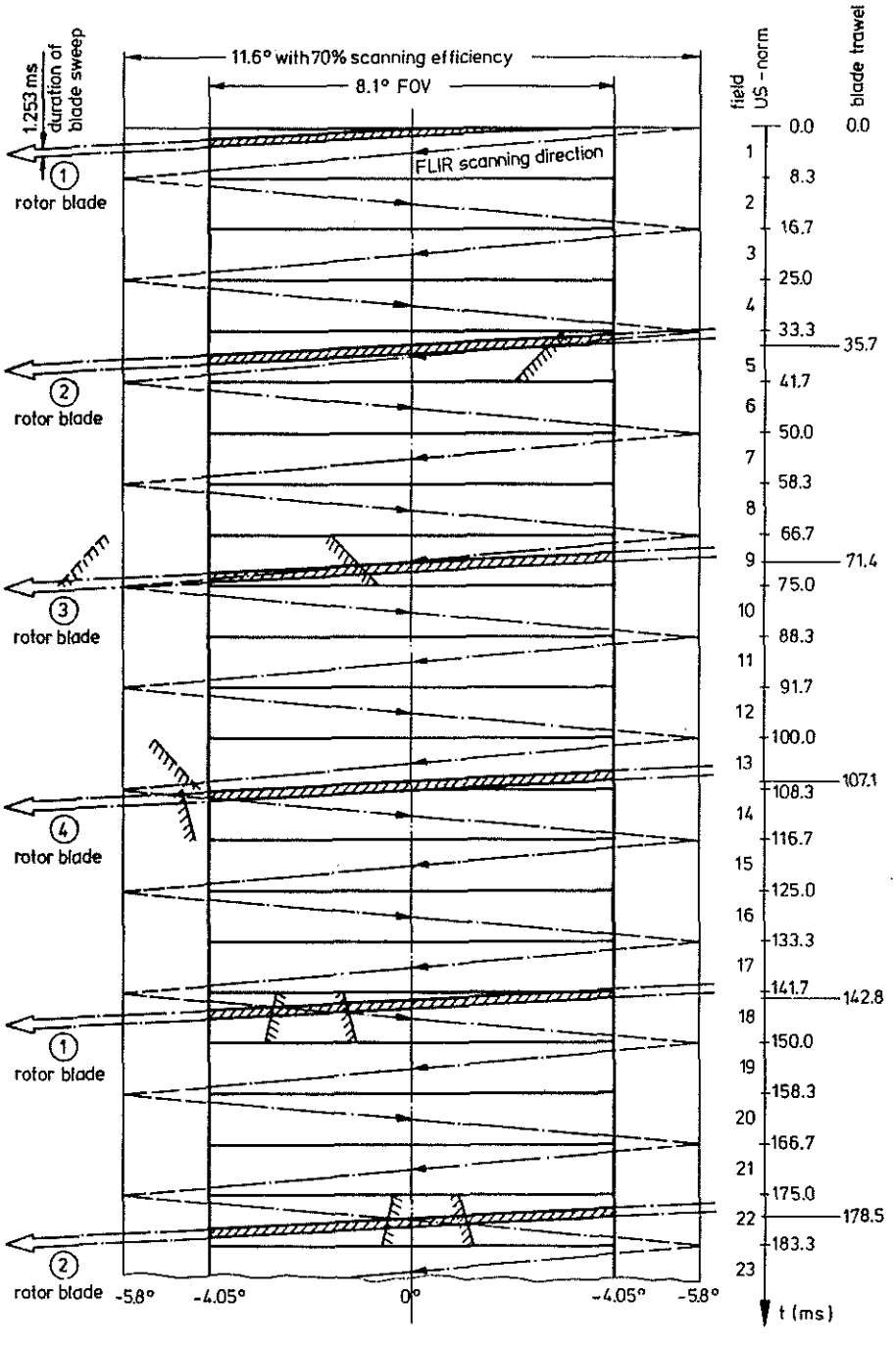

Fig. 19: Dynamic consideration of 23 separate US video fields with rotor blade influence for a mast-mounted CM FLIR with 8.1° x 5.4° FOV.

In the normal case, the rotor blades are not stationary in the centre of the image. Fig. 19 shows a dynamic consideration of 23 separate US video fields (cf. Fig. 14) for a CM FLIR with 8.1° x 5.4° FOV (rotor speed held constant at 2.52°/ms (7 Hz)). After 35.7 ms the 2nd rotor blade appears in the FOV etc. The leading edge of the rotating blade starts at 0.0 ms in the centre of the image in the 1st video field. After 1.253 ms the trailing edge of the blade arrives in the centre of the image. The scanning speed is superimposed on the constant blade rotation. The horizontal scan efficiency of a CM FLIR is 70 %, thus changing the effective FOV width of 8.1° to an apparent FOV width of 11.6°.

In this example, the FLIR scanner starts scanning at 0.0 ms from right to left at - 5.8°. Assuming this, the 2nd rotor blade is shown in the 5th video field. In this video field the rotor blade and the scan mirror rotate in the same direction. This results in the blade image being broadened. Only the trailing edge of the blade is seen in the right-hand part of the 5th video field. The same sense of rotation is maintained in the 9th video field for the 3rd rotor blade. The broadened blade image occurs in the left-hand side of the video field.

The 4th rotor blade does not affect the FLIR FOV. Intersection with the scanner occurs in the dead time between the 13th and the 14th video fields. In the 18th video field, the 1st rotor blade (2nd rotation) and the FLIR scanner rotate in opposite directions. The 1st rotor blade is now compressed. The same effect is seen in the 22nd video field with the 2nd rotation of the 2nd rotor blade. The effect has been demonstrated for 23 separate video fields.

In the dynamic image synthesis of a CM FLIR with rotor blade influence, the effect occurs in a relatively short time scale. Our eyes are not able to perceive these quick processes in detail. A video tape shows these effects much better than any picture or diagram. The eyes can only assimilate the rotor blade influence on a longer time scale by following a random statistic distribution, i.e. acting as a "chopper". With a CM FLIR, no background information is lost in the thermal image during rotor blade influence.

FLIR with serial scanning

The 8-faced polygon in the Honeywell MINI FLIR rotates with approx. 59 000 rev/min or with 63.7°/ms at a FOV width of 8.1° or 90.5°/ms at a FOV width of 11.5°. The horizontal scan efficiency of 42 % is not taken into account. The scanning mechanism in the MINI FLIR operates with either 9 or 14 detectors in line (serial).

In order to produce image synthesis of 249 lines per picture height in 40 ms, very quick scanning must be carried out. The MINI FLIR also cuts the rotor blade image into segments (see CALIPSO FLIR), but these are very small in comparison (one detector line). The step angle of approx. 3° for the LF with 8.1° is much less than that produced by the CALIPSO FLIR. The contours of the rotor blade in a static video field are, however, more markedly blurred than in the CALIPSO FLIR image.

To summarise, we can say that the rotor blades have little influence on the images produced by the various types of mast-mounted FLIR. The observer perceives only a "chopper" effect.

6. Abbreviation

Az	Azimuth
BMFT	Bundesministerium für Forschung und Technologie
CALIPSO	Caméra Légère Infra-rouge Pour Système OPHÉLIA
CCIR	European video standard with 625 lines, 25 Hz frame rate
CM	Common Module (American)
El	Elevation
EP	Entrance Pupil
f_{eff}	effective focal length
FLIR	Forward Looking Infrared
FOV	Field Of View
HDD	Head-down Display
HUD	Head-up Display
IFOV	Instantenous Field Of View
IR	Infrared
LF	Large Field of view
LOS	Line Of Sight
MMO	Mast-Mounted observation platform OPHÉLIA
OPHÉLIA	Optique sur Plate-forme HÉLIcoptère Allemand
SF	Small Field of view
SMT	Système Modulaire Thermique (French Common Module)
TV	Television

7. Reference

(1) H.-D.V. Böhm, B. Behringer — Systembeschreibung und Versuchsauswertung des Rotormast-Sichtsystems OPHÉLIA auf der Bo 105-S1 MBB-TN-DE 235-5/82, April 1982

(2) R.D.v. Reth, M. Kloster — Mast Mounted Visual Aids Seventh European Rotorcraft and Powered Lift Aircraft Forum, Paper No. 53, 8 - 11 Sept. 1981, Garmisch-Partenkirchen, FRG

(3) K. Schymanietz, H.-D.V. Böhm — Nachteinsatz Militärischer Hubschrauber, Analyse und Ausblick 14. Internationales Hubschrauber Forum, Bückeburg 20 - 21 Mai 1982, FRG

(4) H.E. Matuszewski — Helicopter rotor blade effects on mast-mounted sensor images. Subsystems Integration. Bell Helicopter Textron, Fort Worth, Texas 76101, Sept. 1980